Fine Chemical Engineering
http://ojs.wiserpub.com/index.php/FCE/

Research Article

Antimicrobial Activity of Green Synthesized Copper Nanoparticles (CuNPs) Using Aqueous Extract of *Psidium guajava* on Clinical Bacteria Isolates

Mamman Abakeyah James*, Bako Myek, Zakari Ladan

Department of Pure and Applied Chemistry, Faculty of Physical Science, Kaduna State University, Kaduna, Nigeria
E-mail: mammanabakeyah16@gmail.com

Received: 11 December 2023; **Revised:** 26 February 2024; **Accepted:** 7 March 2024

Abstract: The eco-friendly synthesis of nanoparticles using an aqueous plant extract as a capping and stabilizing agent has garnered substantial attention, particularly in pharmaceuticals and drug delivery applications. This study focused on utilizing copper sulfate pentahydrate ($CuSO_4 \cdot 5H_2O$) as a precursor to synthesize copper nanoparticles at both pH 4-5 and pH 8, with *Psidium guajava* (leaves and fruits) extract playing a crucial role. Fourier transform infrared (FTIR) spectroscopy identified four major functional groups at distinct peaks, confirming their responsibility for capping and stabilizing the synthesized *P.g*-CuNPs. Scanning electron microscopy (SEM) revealed spherical shapes with an average particle size range of 20-30 nm. Energy-dispersive X-ray (EDX) analysis confirmed the presence of pure copper (Cu) at 54.15%. The antimicrobial study demonstrated that *P.g*-CuNPs synthesized at pH 4-5 exhibited complete growth inhibition of all tested bacterial strains at varying concentrations. Furthermore, serially diluted *P.g*-CuNPs (pH 5) inhibited *Salmonella spp*, *E. coli*, and *Streptococcus spp* at 100 µg/mL, while *P.g*-CuNPs (pH 8) only inhibited *E. coli* at the same concentration. Notably, acid-based synthesized *P.g*-CuNPs exhibited higher efficacy in the antimicrobial study compared to their alkaline-based counterparts. This study suggests the potential biomedical applications of *P.g*-CuNPs, including therapeutic drugs for microbial infectious diseases, integration into textile coatings, and nanocapsulation for food storage to extend shelf life.

***Keywords*:** copper nanoparticles, *Psidium guajava*, drug-resistant bacteria, green synthesis, *Salmonella spp*, *E. coli*, *S. aureus*, *Streptococcus spp*

1. Introduction

Antimicrobial resistance is a persistent natural occurrence, exacerbated by factors such as excessive and illicit antimicrobial use, inappropriate dosage, sub-therapeutic dosing, and noncompliance with prescribed treatment courses.[1] Nanoparticles have attracted significant attention across diverse domains for their substantial contributions to drug delivery and targeting. They effectively minimize toxicity, enhance efficacy, and create novel avenues for pharmaceutical and drug delivery enterprises.[2-4]

The antimicrobial attributes of bulk metals have been harnessed for millennia. For instance, copper has been utilized for water purification and food preservation since the era of the Persian kings, and copper compounds have

DOI: https://doi.org/10.37256/fce.5120244078

found extensive applications in agriculture, acting as fungistatic agents for grapes and potatoes. In comparison to silver and gold, copper is more cost-effective and readily available. Additionally, copper nanoparticles (CuNPs) exhibit biocompatibility and can be synthesized using environmentally friendly methods.[5]

Several studies have explored the eco-friendly synthesis and antimicrobial activities of copper nanoparticles (CuNPs). For instance, Javier et al.[6] detailed the synthesis, while Amer and Awwad[7] utilized the aqueous extract of Citrus limon fruits for copper nanoparticle synthesis. Other green synthesis methods involved *Punica granatum*,[8] *Prunus mahaleb* L.,[9] and citron juice (*Citrus medica* Linn.).[10] The antimicrobial efficacy of biologically synthesized copper nanoparticles was assessed against *Escherichia coli* and *Staphylococcus aureus*.[11] Biological methods employed plant extracts, bacteria, and fungi,[12] with studies on CuNPs and AgCuNPs targeting udder inflammation pathogens like *Staphylococcus aureus* and *Escherichia coli*.[13]

CuONPs demonstrate heightened antimicrobial efficacy against *E. coli* compared to *S. aureus*. Spherical CuONPs (33 nm) and CuO nanosheets (257 × 42 nm) completely inhibit the growth of Gram-negative bacteria *Proteus vulgaris* and *E. coli* at concentrations of 0.16 and 0.20 mg/mL, respectively. Furthermore, these nanomaterials inhibit the growth of Gram-positive bacteria *Bacillus subtilis* and *Micrococcus luteus* at concentrations of 0.22 and 0.20 mg/mL, respectively.[14] At a higher concentration of CuNPs (3,200 μg/mL), inhibition of *S. aureus* and *P. aeruginosa in vitro* surpasses 99%. Moreover, 800 nm Cu_2O@ZrP hybrid nanosheets exhibit significant efficacy, achieving a 99% reduction after 6 hours against methicillin-resistant *Staphylococcus aureus* (MRSA) and vancomycin-resistant *Enterococcus* (VRE).[15-17]

Plants have a long history of being recognized for their therapeutic attributes, with aboriginal cultures globally utilizing traditional herbal medicine for centuries.[18] The recent surge in demand for herbal medicines is attributed to their efficacy with minimal side effects.[19] Concerns about the adverse effects, therapeutic complexities, and cost implications of modern medicines, such as chemotherapy, hormone-blocking therapy, and monoclonal antibodies, have prompted a turn towards ethnopharmacological remedies.[20] Ethnopharmacology serves as an approach to identify potential medicinal compounds by evaluating plants with therapeutic potential.[21] Throughout history, plants and their secondary metabolites have consistently served as an exemplary source of medicine, renowned for their antibacterial and anticancer effects.[22]

Figure 1. *Psidium guajava* plant showing leaves and fruit

Psidium guajava, commonly referred to as guava, originates from the Caribbean and Central and South America, thriving as a tropical fruit-bearing tree within the Myrtaceae family.[23] Guava is known for its delectable and consumable produce as shown in Figure 1, rich in dietary fiber, essential vitamins A and C, folic acid, and dietary minerals like potassium, copper, and manganese.[11] Guava fruits and leaves contain a high amount of vitamins, tannins, polyphenols, and various compounds, including resin, sugars, triterpenes, essential oil, isoquercitrin, reynoutrin, guajaverin, avicularin, kaempferol, guajanoic acid, saponin, carotenoids, lectins, leucocyanidin, ellagic acid, amritoside, β-sitosterol,

uvaol, oleanolic acid, and ursolic acid.[24-25] Pharmacological research, both *in vitro* and *in vivo*, on guava leaves, has demonstrated their potential for co-treating various ailments, including infectious and parasitic diseases, neoplasms, blood and immune system disorders, endocrine and metabolic diseases, circulatory system disorders, digestive system disorders, and skin-related issues. Furthermore, several randomized and clinical trials conducted in the last two decades have explored the effects of guava leaf extract in treating various medical conditions.[26-27]

Capping agents play a crucial role in functionalizing and stabilizing synthesized nanoparticles, serving as biologically acceptable reducing, stabilizing, or capping agents. These agents are carefully chosen to ensure compatibility with the living systems.[28-29] They play a pivotal role in shielding nanoparticles from agglomeration and enhancing reduction kinetics by forming complex structures with metallic ions in precursor salts.[30-31]

Shakeela and colleagues have highlighted the pivotal role of pH in nanoparticle (NP) synthesis. They pointed out that higher pH levels lead to the production of smaller NPs, hindering further nucleation, while acidic pH impedes NP formation, and alkaline pH facilitates it.[32-33] Saliani et al.[34] observed that the inhibitory effects of NPs on bacterial growth are pH-dependent, with growth inhibition intensifying as pH decreases from 7 to acidic levels.[34] Given the established antimicrobial activity of *Psidium guajava* extracts and the pH-dependent microbial growth inhibition, the synthesis of CuNPs at a pH range of 4-5 using these plant extracts emerges as a promising strategy to address challenges associated with antimicrobial resistance (AMR). Notably, there is no existing literature over the past ten years on biosynthesizing copper nanoparticles using *Psidium guajava* aqueous extract at acidic pH and testing its antimicrobial activity on clinical resistant strains of *Salmonella spp*, *Escherichia coli*, *Staphylococcus aureus*, and *Streptococcus spp*.

As a result, this study aims to synthesize and characterize copper nanoparticles using the aqueous extracts of *Psidium guajava* (leaves combined with fruits) and to conduct antimicrobial tests on clinical resistant isolates of two gram-negative bacteria (*Salmonella spp* and *Escherichia coli*) and two gram-positive bacteria (*Staphylococcus aureus* and *Streptococcus spp*). Our objective is to perform both acidic and alkaline syntheses of CuNPs and compare their antimicrobial activity on resistant clinical isolates.

2. Materials and methods

2.1 *Collection and identification of plant extract and bacteria isolates*

Psidium guajava leaves and fruits were collected at Chikun LGA, Kaduna, Nigeria, and authenticated by a taxonomist at the Department of Biological Science Herbarium, Ahmadu Bello University, Zaria, Kaduna, Nigeria, with voucher numbers V/N-ABU3253. Clinical isolates of *Staphylococcus aureus* (Urine), *Streptococcus spp* (Sputum), *Salmonella spp* (Stool), *Escherichia coli* (Urine), and *Staphylococcus aureus* (High Vaginal Swab) were collected at Oxford Hospital Chemical Pathology, Hematology, and Microbiology diagnostic laboratory Makera, Kakuri, Kaduna State, Nigeria.

2.2 *Preparation of aqueous copper sulfate pentahydrate ($CuSO_4{\cdot}5H_2O$)*

A 0.1 M $CuSO_4{\cdot}5H_2O$ (Kermel minimum assay 99.0%) solution was prepared by weighing 2.496 g of $CuSO_4{\cdot}5H_2O$ using an analytical balance and dissolving it in distilled water to the 100 mL mark of a 100 mL volumetric flask.

2.3 *Preparation of aqueous Psidium guajava extract and CuNPs synthesis*

The method of Chhangte et al.[35] was adopted with slight modifications. Twenty grams of *Psidium guajava* leaves and fruit were weighed, sliced into small pieces with a knife, and gently pounded using a mortar and pestle. 100 mL of distilled water was added to the extract, and more of its juice was filtered with Whatman No. 1 filter paper and set aside for copper nanoparticles synthesis as a stabilizing and capping agent. 30 mL of the filtrate was added to 70 mL of 0.1 M solution of $CuSO_4{\cdot}5H_2O$ in a 100 mL conical flask set on a hot plate at 70 °C. While stirring, a drop of H_2SO_4 was added to adjust the pH to 4-5, and the stirring continued until the color changed from green to pale blue, confirming the synthesis of green CuNPs. The green-synthesized *P.g*-CuNPs were then subjected to centrifugation to obtain colloidal particles. After eliminating the supernatant, it was oven-dried at 40 °C. The same procedure was carried out for alkaline synthesis of CuNPs at pH 8 using NaOH for pH adjustment (see Figure 2). The acidic copper nanoparticles were

characterized using a combination of spectroscopic techniques: UV-Vis, FTIR, SEM, and EDX.

Figure 2. A: $CuSO_4 \cdot 5H_2O$, B: *P. guajava* extract, C: Before synthesis, D: *P.g*-CuNPs after synthesis at pH 5, E: *P.g*-CuNPs after synthesis at pH 8

2.4 *Characterization of green-synthesized nanoparticles*

Ultraviolet and visible spectrophotometer (UV-Vis) was employed to monitor the synthesis of CuNPs. The blank, consisting of distilled water, and the prepared nanoparticle solution underwent successive dilutions with distilled water before being placed in a quartz cuvette. The scanning procedure covered a range from 200 to 800 nm.[36]

For FTIR analysis, the Agilent surface-sensitive attenuated total reflection Fourier transform infrared technique (ATR-FTIR) instrument underwent calibration, and a small amount of the sample was placed onto the ATR crystal surface for measurement. The obtained infrared spectrum reflected the absorption of infrared light by the functional groups within *Psidium guajava* extracts and the synthesized copper nanoparticles, respectively.[37]

In SEM examination, uncontaminated nanoparticles in a dry state were evenly distributed on an appropriate substrate. The SEM apparatus was activated, and imaging parameters were configured to capture SEM images, illustrating the morphology and surface characteristics of the nanoparticles.[38]

For energy dispersive X-ray (EDX) analysis, the EDX mode was activated with meticulous detector configuration. Regions of interest designated on SEM images facilitated EDX analysis for element identification and quantification of their relative abundance. The obtained EDX spectra were analyzed via specialized software to discern elements and approximate concentrations. Results were then compared with SEM images to elucidate the elemental distribution on the nanoparticle surface.[39]

2.5 *Antimicrobial screening*

The antimicrobial screening involved the Kirby-Bauer disk diffusion test, utilizing Mueller-Hinton Agar (MHA) following the protocol described by Olgica et al.[40] Sterilization of the area and inoculation of bacterial colonies onto the agar plate were conducted under aseptic conditions.[10] After the application of antimicrobial disks and incubation, the plates were examined for the zone of inhibition around each disk. The diameter of these zones was measured, indicating susceptibility or resistance.[10]

In the antimicrobial susceptibility tests for *Psidium guajava* extract and *P.g*-CuNPs, confirmed clinical isolates were utilized, and specific concentrations of the prepared samples were tested against various bacterial strains.

2.5.1 *For Psidium guajava extract and P.g-CuNPs*

The antimicrobial susceptibility tests were conducted for confirmed clinical isolates using the following prepared samples:

For *P. guajava*

• d for 1 mg/mL Guava extract;
• 0 for 0.1 mg/mL CuNPs;
• 1 for 0.25 mg/mL CuNPs;
• 3 for 0.5 mg/mL CuNPs.

2.5.2 *For serial diluted Psidium guajava extract and P.g-CuNPs*

The antimicrobial susceptibility tests were conducted for confirmed clinical isolates using the following serially diluted prepared samples:

For *P. guajava*

• X and Y for 10 and 100 µg/mL plant extract;
• A and B for 10 and 100 µg/mL CuNPs at pH 4-5;
• 1 and 2 for 10 and 100 µg/mL CuNPs at pH 8.

3. Results and discussions

3.1 *Synthesis of CuNPs*

When *P. guajava* leaf/fruit extract was mixed with $CuSO_4 \cdot 5H_2O$ solution, heated at 60 °C for 10 minutes, and acidified, a color change from green to pale blue occurred, indicating the synthesis of copper nanoparticles. The Surface Plasmon Resonance phenomenon in copper nanoparticles and electrostatic interactions and hydrogen bonds between biogenic capping molecules were responsible for the synthesis.[36] This color change was consistent with literature reports indicating the completion of the reduction process within 24 hours.[11]

The UV-Vis spectrum (Figure 3) displayed absorbance peaks at λmax 352 nm, indicative of CuNPs, which aligns with the findings reported by Wu et al.[41] In their investigation on the green synthesis of copper nanoparticles using *Cissus vitiginea*, they observed a broadened surface plasmon resonance (SPR) peak at λmax 340 nm in the UV-Vis spectrum, confirming the synthesis of polydispersed nanosized particles, a characteristic feature of copper nanoparticles. Similarly, Caroling et al.,[11] in their study on the biosynthesis of copper nanoparticles using aqueous guava extract, noted distinct surface plasmon resonance bands with a peak at λmax 350 nm after 24 hours at pH 6. Additionally, Yilleng et al.,[36] in their research on the biosynthesis of copper and iron nanoparticles using neem (*Azadirachta indica*) leaf extract, reported a strong peak at 250 nm with an absorbance of 2.718, attributed to the formation of copper nanoparticles.

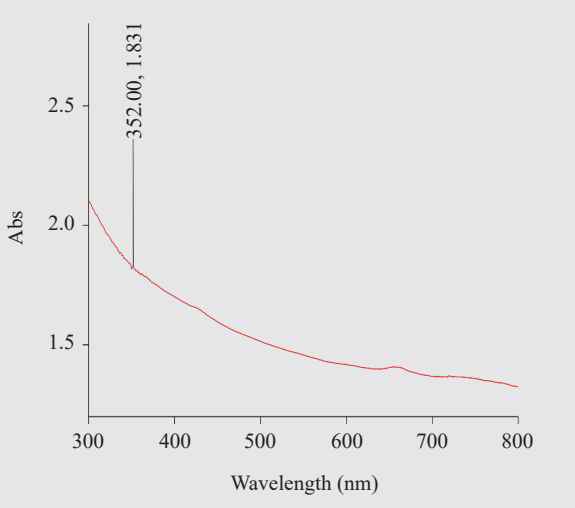

Figure 3. UV spectrum of *P.g*-CuNPs

Figure 4. ATR-FTIR of aqueous *P. guajava* extract

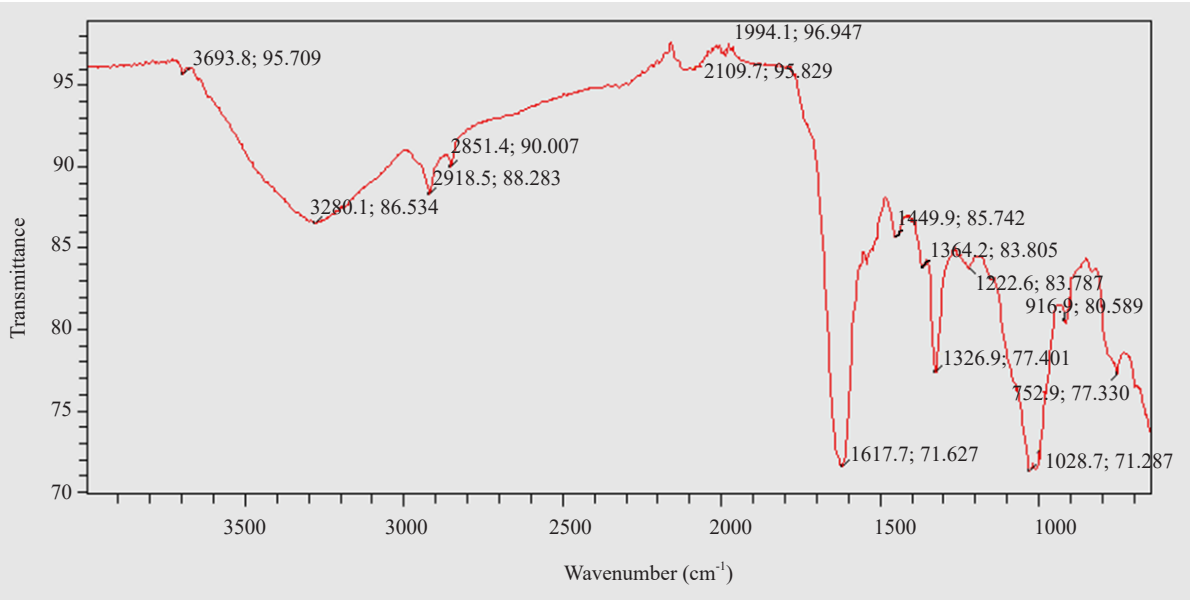

Figure 5. ATR-FTIR of *P. guajava*-CuNPs

3.2 *ATR-FTIR spectroscopy of P. guajava extract and synthesized P.g-CuNPs*

The ATR-FTIR spectroscopy results of *P. guajava* extract and the synthesized *P.g*-CuNPs are depicted in Figures 4 and 5. Characteristic peaks in the *P. guajava* extract were observed at 3,693 cm^{-1}, 3,280 cm^{-1}, 2,918 cm^{-1}, 2,851 cm^{-1}, 2,109 cm^{-1}, 1,884 cm^{-1}, 1,617 cm^{-1}, 1,449 cm^{-1}, 1,364 cm^{-1}, 1,326 cm^{-1}, 1,222 cm^{-1}, 1,028 cm^{-1}, 916 cm^{-1}, and 752 cm^{-1}. The peaks from 3,693 cm^{-1} to 2,600 cm^{-1} were attributed to single bonds of N-H stretching, O-H stretching, and C-H stretching, in line with previous studies.[11,41] Bands between 3,600 and 3,200 cm^{-1} were associated with O-H stretching from phenol, N-H stretching from amide, and C-H stretching at 3,000-2,840 cm^{-1}. Peaks from 2,110 cm^{-1} to 1,415 cm^{-1} were assigned

to double bonds of C=C, C=N, C=C=C, C=O, and cyclic carbon (C=C), as well as triple bonds of C≡C and C≡N stretching vibration.[11,36,42-43] Similar peaks were reported within the range of 2,110 to 1,635 cm^{-1}, associated with C=C, C=N, C=C=C, C=O, aromatic (C=C), C≡C, and C≡N stretching vibration. Peaks from 1,368 cm^{-1} to 752 cm^{-1} were attributed to C-O stretching, -CH_2- bending vibrations, and alkyl halides,[36,42,44] with reported peaks from 1,330 cm^{-1} to 720 cm^{-1} associated with C-O stretch, -CH_2- bending vibrations, and alkyl halides.

The *P. guajava* extract copper nanoparticles (*P.g*-CuNPs) exhibit only four distinct peaks. The peak at 3,235.3 cm^{-1} is attributed to O-H stretch or terminal ≡C-H stretch, while the peak at 2,109.7 cm^{-1} is associated with C≡C, C≡N stretching vibrations. Additionally, the peak at 1,640.0 cm^{-1} corresponds to C=C stretching for alkene, and the peak at 1,069.7 cm^{-1} corresponds to C-O stretch. Figure 5 illustrates variations in the wave numbers of these peaks in *P.g*-CuNPs, potentially resulting from conjugation induced by synthesis temperature and/or the addition of concentrated sulfuric acid. Notably, the peak at 2,109.7 cm^{-1} remains unaffected by the reaction. In contrast, several functional groups present in the *P. guajava* extract, as depicted in Figure 4, are absent in *P.g*-CuNPs. The missing functional groups, along with those exhibiting decreased and increased wavenumbers, likely play roles in the reduction, capping, and stabilization of the synthesized copper nanoparticles, aligning with Javed and co-workers.[28,45] The latter authors reported that plant extracts, containing phytometabolites like phenols and flavonoids, act as stabilizing or reducing agents in the copper salt reduction process.[45-46]

3.3 *Scanning electron microscope (SEM) micrographs and energy dispersive X-ray (EDX) analysis of synthesized P.g-CuNPs*

Figure 6 displays SEM micrographs of the synthesized *P.g*-CuNPs, revealing predominantly spherical nanoparticles with an average size of 20-30 nm. The non-uniform distribution and agglomeration of nanoparticles may be attributed to the precursor concentration and biomolecules in *P. guajava* leaf extracts, as well as the presence of secondary metabolites in leaves and fruit extracts. This observation aligns with Amer and Awwad,[7] who reported a similar outcome in their study on green synthesis of copper nanoparticles using Citrus limon fruit extract. They observed spherical CuNPs with an average diameter of 28 nm. Nasrollahzadeh et al.[47] also found spherical CuNPs (7-35 nm) in their study on green synthesis using *Plantago asiatica* leaf extract, while Mostafa,[48] reported spherical particle sizes ranging from 22-27 nm in his review on biogenic copper nanoparticles and their applications.

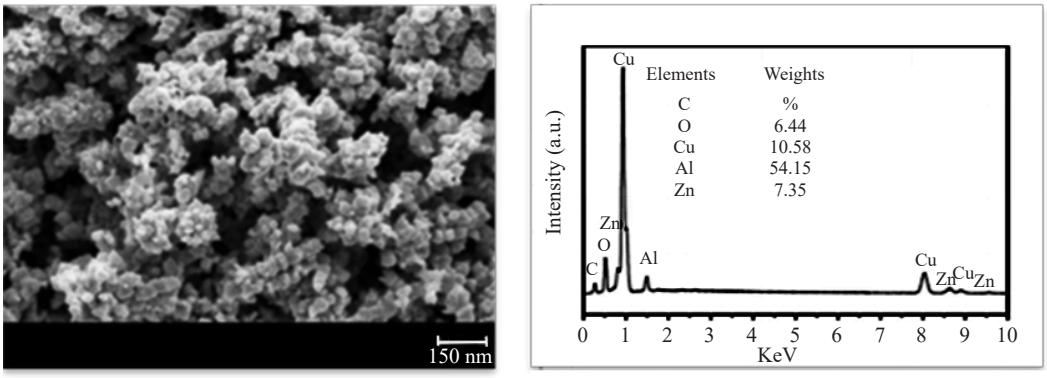

Figure 6. SEM-EDX analysis of *P.g*-CuNPs

Energy dispersive X-ray (EDX) analysis was conducted to ascertain the elemental composition of the synthesized *P.g*-CuNPs presented in Figure 6. The results revealed the presence of pure copper (Cu) at a significant proportion of 54.15%, detected at energy levels of 1, 8, and 9 keV. This robust signal in the metallic copper region serves as confirmation of the successful formation of copper nanoparticles using *P. guajava*. Additionally, peaks were observed for other elements, including aluminum (Al) at 21.47%, oxygen (O) at 10.58%, zinc (Zn) at 7.35%, and carbon (C) at

6.44%. Notably, a substantial percentage of aluminum atoms were noted on the surface of *P.g*-CuNPs nanoparticles, possibly originating as an impurity from the precursor or from agricultural chemicals used on the *P. guajava* plant, sourced from a farm.

Comparably, a study by Ahmed et al.[49] reported similar outcomes in EDX analysis, where copper nanoparticles synthesized using leaf extract of *Camellia sinensis* exhibited a predominant copper content (48.89%), along with elements such as oxygen (21.24%), chlorine (12.7%), and carbon (9.69%), among others. Wu et al.[41] also observed various elemental constituents in copper nanoparticle synthesis using leaves of the same plant.

3.4 *Antimicrobial assay*

The antimicrobial assay of *P. guajava* extracts and *P.g*-CuNPs is presented. Table 1 and Figure 7 display the results of the antimicrobial susceptibility test. Both *P. guajava* extracts and *P.g*-CuNPs, when applied as prepared disks at all concentrations, exhibited positive inhibition against four tested bacterial strains (*Salmonella spp*, *S. aureus*[A] [Urine], *S. aureus*[B] [High vaginal swab], and *Streptococcus spp*). The inhibitory effects were so pronounced that the inhibition zone could not be determined (CND) due to the acidic pH and the concentration of *P.g*-CuNPs.

Table 1. Zone of inhibition of *P. guajava* synthesized copper nanoparticles *P.g*-CuNPs

Bacteria isolates	Diameter of inhibition zone (mm)			
	Guava extract	Guava extract copper nanoparticles, AgNPs		
	1 mg/mL	0.1 mg/mL	0.25 mg/mL	0.5 mg/mL
Salmonella spp	CND	CND	CND	CND
S. aureus[A]	CND	CND	CND	CND
S. aureus[B]	CND	CND	CND	CND
Streptococcus spp	CND	CND	CND	CND

A: Urine, B: High vaginal swab, CND: Cannot be determine

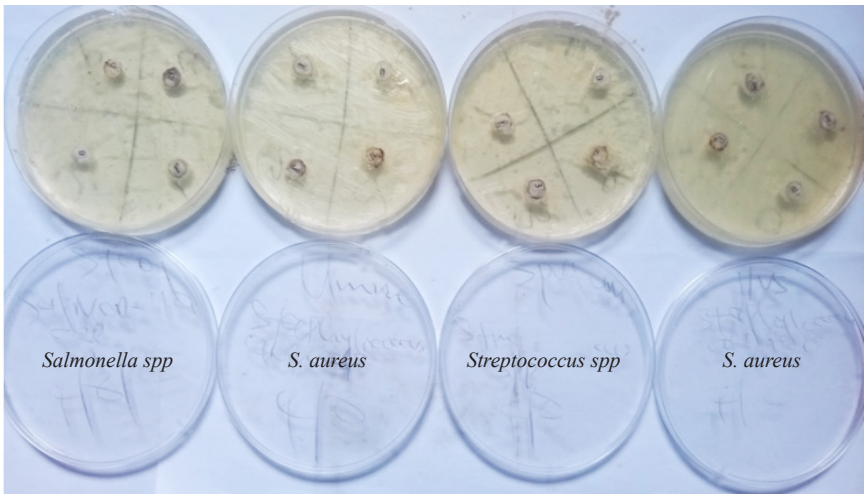

Figure 7. Antimicrobial susceptibility test of CuNPs at acidic pH

It has been documented that an increase in the concentration of CuNPs corresponds to an escalation in antibacterial activity, establishing a clear direct proportionality between concentration and antibacterial effectiveness.[50] Similarly, Aleksandra et al.[13] proposed that the toxicity of CuNPs is influenced by various factors, including temperature, aeration, pH, and bacteria concentration.

Moreover, elevated temperature, improved aeration, and low pH conditions enhance the toxicity of CuNPs by minimizing agglomeration, resulting in a greater surface area available for interaction with bacterial cell membranes. Bio-capped copper nanoparticles produce reactive oxygen species (ROS), which interact with bacterial cell membranes, leading to penetration into the cell. This intrusion disrupts the cell membrane, inhibiting bacterial cell growth and potentially causing cell death.[45]

Table 2. Zone of inhibition of serial diluted *P. guajava* synthesized copper nanoparticles *P.g*-CuNPs

Bacteria isolates	Diameter of inhibition zone (mm)					
	P. guajava extract		CuNPs (pH 5)		CuNPs (pH 8)	
	X 10 µg/mL	Y 100 µg/mL	A 10 µg/mL	B 100 µg/mL	1 10 µg/mL	2 100 µg/mL
Salmonella spp	0 mm	0 mm	0 mm	10 mm	0 mm	0 mm
S. aureus	0 mm	0 mm	0 mm	0 mm	0 mm	0 mm
E. coli	0 mm	0 mm	0 mm	7 mm	0 mm	6 mm
Streptococcus spp	0 mm	0 mm	0 mm	6 mm	0 mm	0 mm

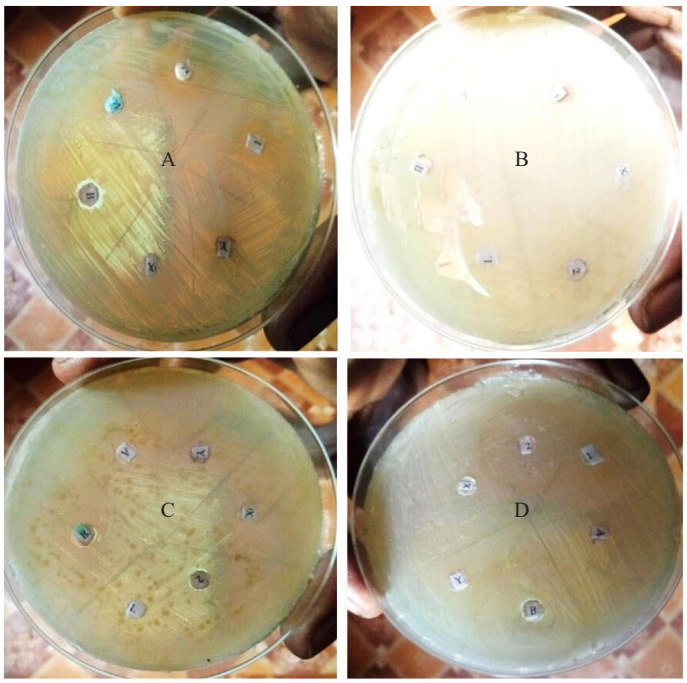

Figure 8. Antimicrobial susceptibility test of *P. guajava* extract, *P.g*-CuNPs (pH 5) and *P.g*-CuNPs (pH 8)

3.5 *Antimicrobial assay of serially diluted P. guajava extracts and P.g-CuNPs*

Table 2 and Figure 8 depict the antimicrobial susceptibility test for *P. guajava* extracts and *P.g*-CuNPs prepared disks. At concentrations of 10 µg/mL and 100 µg/mL, *P. guajava* extracts exhibited no inhibition against the four tested bacterial strains. This lack of inhibition can be attributed to the serial dilution, resulting in lower concentrations of the *P. guajava* extract. Plant extracts typically require higher concentrations to demonstrate positive inhibition against bacteria, and even higher concentrations may be necessary for resistant bacteria.

Additionally, *P.g*-CuNPs at a pH of 5 and 8, both at a concentration of 10 µg/mL, exhibited no inhibitory effects on the tested bacterial strains, namely *Salmonella spp*, *S. aureus*, *E. coli*, and *Streptococcus spp*. This lack of inhibition can be attributed to the specific nature of these bacterial strains, requiring a higher concentration of the synthesized copper nanoparticles for effective inhibition. Similar findings were reported by Dashtizadeh et al.,[9] where CuNPs showed no zone of inhibition (ZOI) against various bacteria and yeast strains.

In contrast, *P.g*-CuNPs at a pH of 8, when tested at a concentration of 100 µg/mL, demonstrated positive inhibition only against *E. coli* with a ZOI of 6 mm. On the other hand, *P.g*-CuNPs at a pH of 5, at the same concentration, exhibited positive inhibition with ZOI values of 10 mm, 7 mm, and 6 mm for *Salmonella spp*, *E. coli*, and *Streptococcus spp*, respectively. This increased inhibitory effect is attributed to the higher concentration of *P.g*-CuNPs.

Consistent with these observations, Reda et al.[50] noted in their study on the biosynthesis of copper nanoparticles that increasing concentrations (A = 25, B = 50, C = 100, and D = 200 µg/mL) resulted in enhanced antibacterial activity. This finding supports the direct proportionality between nanoparticle concentration and antibacterial efficacy, as highlighted by Reda and colleagues Reda et al.[50] It was also reported that copper nanoparticles attach to the cell membrane, disrupting its function and directly interacting with the bacterial outer membrane, leading to the release of Cu ions.[11] The high reactivity of copper nanoparticles, owing to their elevated surface area to volume ratio, facilitates extensive interaction with the cell membrane, causing damage to cellular genetic materials and ultimately inducing cell death.[51]

4. Conclusion

In conclusion, this study demonstrated the bio-reduction of aqueous copper ions by the leaf/fruit extract of the *P. guajava* plant under both alkaline and acidic conditions. The resulting copper nanoparticles, characterized through UV-Vis, ATR-FTIR, SEM, and EDX analyses, displayed an average particle size of 20-30 nm. Notably, the UV-Vis spectrum exhibited a characteristic peak at 352 nm, and EDX confirmed the presence of pure copper (54.15%). ATR-FTIR revealed distinct peaks for *P.g*-CuNPs, with the peak at 2,109.7 cm^{-1} remaining consistent with the *Psidium guajava* FTIR spectrum, suggesting the reduction, capping, and stabilization of synthesized *P.g*-CuNPs through a green synthesis approach.

The antimicrobial efficacy of the synthesized *P.g*-CuNPs was evident, with complete inhibition of tested bacteria at concentrations of 0.1, 0.25, and 0.5 mg/mL at pH 4-5. Furthermore, serially diluted *P.g*-CuNPs at pH 5 demonstrated inhibitions against *Salmonella spp*, *E. coli*, and *Streptococcus spp* at 100 µg/mL, while those at pH 8 inhibited only *E. coli* at the same concentration. Notably, acid-based synthesized *P.g*-CuNPs outperformed their alkaline counterparts, attributed to the lower pH and unfavorable conditions for bacterial survival in an acidic medium. The maximum zone of inhibition was observed in gram-negative bacteria, highlighting the antibacterial activity of *P.g*-CuNPs at pH 5 compared to pH 8.

In light of these findings, *P.g*-CuNPs derived from *Psidium guajava* hold promising applications in various biomedical fields, serving as therapeutic drugs for enhanced efficacy against microbial infectious diseases. Additionally, their incorporation into textile coatings can add antimicrobial properties, and nanocapsulation for use in food storage can potentially extend the shelf life of food items.

Acknowledgments

The authors express their gratitude for the assistance in the antimicrobial analysis provided by Mr. Samuel from the

Department of Chemical Pathology, Hematology, and Microbiology Diagnostic Laboratory at Oxford Hospital Makera, Kakuri, Kaduna State, Nigeria. The authors also acknowledge the valuable suggestions from the peer reviewers.

Ethics approval

The ethical permit was obtained from the Ministry of Health in Kaduna State, Nigeria, and was strictly adhered to from sampling the clinical isolates to the antimicrobial test.

Conflict of interest

The authors declare no competing financial interest.

References

[1] Centers for Disease Control and Prevention (CDC). https://www.cdc.gov/drug resistance/biggest-threats.html (accessed Nov 22, 2019).
[2] Jokerst, J. V.; Jeanne, E. L.; Hartanto, J. *Trends Anal. Chem*. **2017,** *97*, 445-458.
[3] Lutfi, G.; Gokhan, D.; Gamze, G. *J. Mat. Sci. Engr*. **2011,** *1*, 132-133.
[4] Blanco, E.; Shen, H.; Ferrari, M. *Nat. Biotech*. **2015,** *33*, 941-951.
[5] Ermini, M. L.; Voliani, V. *ACS Nano*. **2021,** *15*, 6008-6029.
[6] Javier, S.; Heriberto, E.; Gabrie, A.; Ignacio, A. R.; Yadira, G.; Lucía, Z. F. *J. Saudi Chem. Soc*. **2017,** *21*, 341-348.
[7] Amer, M. W.; Awwad, A. M. *Chem. Int*. **2021,** *7*, 1-8.
[8] Padma, N. P.; Syed, T. B.; Chaitanya, K. S. *Annual Res. Rev. Bio*. **2018,** *23*, 1-10.
[9] Dashtizadeh, Z.; Fereshteh, J. K.; Mahdi, A. *Mats. Tod. Comm*. **2021,** *27*, 102456.
[10] Sudhir, S.; Avinash, P. I.; Aniket, G.; Mahendra, R. *World J. Microbio. Biotech*. **2015,** *15*, 1840.
[11] Caroling, G.; Nithya, P. E.; Vinodhini, M.; Mercy, R. A.; Shanthi, P. *Int. J. Pharm. Bio. Sci*. **2015,** *5*, 25-43.
[12] Muhammad, I. D.; Rida, R. *Anal. Lett*. **2017,** *50*, 50-62.
[13] Aleksandra, K.; Sławomir, J.; Mateusz, W.; Marcin, G. *Int. J. Mol. Sci*. **2019,** *20*, 16-72.
[14] Laha, D.; Pramanik, A.; Laskar, A.; Jana, M.; Pramanik, P.; Karmakar, P. *Mater. Res. Bull*. **2014,** *59*, 185-191.
[15] Applerot, G.; Lellouche, J.; Lipovsky, A.; Nitzan, Y.; Lubart, R.; Gedanken, A.; Banin, E. *Small*. **2012,** *8*, 3326-3337.
[16] Betancourt-Galindo, R.; Reyes-Rodriguez, P. Y.; Puente-Urbina, B. A.; Avila-Orta, C. A.; Rodríguez-Fernández, O. S.; Cadenas-Pliego, G.; Lira-Saldivar, R. H.; García-Cerda, L. A. *J. Nanomater*. **2014,** *2014*, 980545.
[17] Zhou, J.; Xiang, H.; Zabihi, F.; Yu, S.; Sun, B.; Zhu, M. *Nano Res*. **2019,** *12*, 1453-1460.
[18] Li, F. S.; Weng, J. K. *Nat. Plants.* **2017,** *3*, 17109.
[19] Priyanka, P.; Brahmeshwar, M. *J. Pharm. Res*. **2017,** *16*, 86.
[20] Tanmoy, S.; Buddhadev, L.; Swayam, P. *Drug Delivery Transl. Res*. **2017,** *17*, 1-12.
[21] Tita, J.; Iis, S. J.; Ida, D.; Elvira, H.; Yaya, R. *Rasayan J. Chem*. **2020,** *13*, 1096-1103.
[22] Maya, S. N.; Soren, K.; Singh, V.; Boro, B. *Austin J. Pharm. Ther*. **2016,** *4*, 1082.
[23] Singh, R. K.; Kumar, R. *J. King Saud Uni-Sci*. **2021,** *33*, 101-107.
[24] Rayjade, M. S.; Bhambar, R. S.; Attarde, D. L. *J. Pharm. Sci. Res*. **2021,** *13*, 406-411.
[25] Yaun, E. A.; Vasquez, B. A. *J. Res. Univ. Visayas*. **2017,** *11*, 1-6.
[26] Biswas, B.; Rogers, K.; McLaughlin, F.; Daniels, D.; Yadav, A. *Int. J. Microbiol*. **2013,** *7*, 746165.
[27] Díaz-de-Cerio, E.; Verardo, V.; Gómez-Caravaca, A. M.; Fernández-Gutiérrez, A.; Segura-Carretero, A. *Int. J. Mol. Sci*. **2017,** *18*, 897.
[28] Javed, R.; Zia, M.; Naz, S.; Aisida, S. O.; ul Ain, N.; Ao, Q. *J. Nanobiotech*. **2020,** *18*, 1-15.
[29] Ocsoy, I.; Tasdemir, D.; Mazicioglu, S.; Celik, C.; Kat, A.; Ulgen, F. *Mat. Lett*. **2018,** *212*, 45-50.
[30] Sharma, P.; Kumari, S.; Ghosh, D.; Yadav, V.; Vij, A.; Rawat, P. *Mat. Chem. Phy*. **2021,** *258*, 123899.
[31] Campisi, S.; Schiavoni, M.; Chan-Thaw, C. E.; Villa, A. *Rec. Adv. Pers. Cat*. **2016,** *6*, 185.
[32] Shakeela, L.; Abram, M.; Mervin, M. *Green Synthesis and Characterization of Silver Nanoparticles (AgNPs) from Bulbine Frutescens Leaf Extract and Their Antimicrobial Effects*; University of the Western Cape, Bellville Press:

South Africa, 2019; pp 27-30.
[33] Sithole, Z. N. Synthesis of silver nanoparticles and investigating their antimicrobial effects. University of the Western Cape. Master Thesis, 2015.
[34] Saliani, M.; Razieh, J.; Elaheh, K. G. *Jundishapur J. Microbial*. **2015,** *8*, 17115.
[35] Chhangte, V.; Samuel, L.; Ayushi, B.; Manickam, S.; Bishwajit, C.; Samuel, L. R. *RSC Adv*. **2021,** *11*, 2804.
[36] Yilleng, T. M.; Samuel, N. Y.; Stephen, D.; Akande, J. A.; Agendeh, Z. M.; Madaki, L. A. *J. Appd. Sci. Envi. Mngt*. **2020,** *24*, 1987-1991.
[37] Gideon, M. *INNOSC Theranostics Pharm. Sci*. **2023,** *5*, 27-34.
[38] Kalu, A. O.; Egwim, E. C.; Jigam, A. A.; Muhammed, H. L. *Nano Exp. Papers*. **2022,** *3*, 045004.
[39] Kithokoi, K. J.; Wilson, N.; Sauda, S. *Silver Nanoparticles and Their Antibacterial Activity Synthesized Using Selected Medicinal Plant Extracts*; Kenyatta University Press, 2019; pp 22-79.
[40] Olgica, D. S. Synergistic activity of antibiotics and bioactive plant extracts: A study against gram-positive and gram-negative bacteria. In *Bacterial Pathogenesis and Antibacterial Control*; IntechOpen, 2018.
[41] Wu, S.; Shanmugam, R.; Malini, M.; Vanaja, M. *Artif. Cells Nanomed. Biotechnol*. **2020,** *48*, 1153-1158.
[42] Félix, Z.; Adrián, L.; Fernando, O.; Gloria, Q.; Carmen, G.; Gemma, M. *J. Chem. Edu*. **2021,** *98*, 2675-2686.
[43] Monowar, T.; Rahman, M. S.; Bhore, S. J.; Sathasivam, K. V. *Pharmaceutics*. **2021,** *13*, 511.
[44] Ibrahim, A. H.; Nader, A. S.; Gade, C. K.; Amanda, G. H.; Nammalwar, S.; Eugene, G. J.; Roop, L. M. *Fabric. Self-Assem. Nanobiomat*. **2016,** *323*, 1-8.
[45] Rakshit, S.; Paresh, C. J.; Tapanendu, K. *Curr. Nanomater*. **2023,** *8*, 110-125.
[46] Das, P. E.; Abu-Yousef, I. A.; Majdalawieh, A. F.; Narasimhan, S.; Poltronieri, P. *Molecules*. **2020,** *25*, E555.
[47] Nasrollahzadeh, M.; Momeni, S. S.; Sajadi, S. M. *J. Coll. Interf. Sci*. **2017,** *506*, 471-477.
[48] Mostafa, F. A. Biogenic copper nanoparticles and their applications: A review. *SN Appl. Sci*. **2020,** *2*, 505.
[49] Ahmed, A.; Muhammad, U.; Qian-Ying, L.; You-Qing, S.; Bing, Y.; Hai-Lin, C. *Ferroelectrics*. **2019,** *549*, 61-69.
[50] Reda, H.; Dalal, Z. H.; Mostafa, F. A. *Heliyon*. **2018,** *4*, e01077.
[51] Rajeshkumar, S.; Soumya, M.; Venkat, K. S.; Murtaza, M. T.; Hamid, A. B.; Meenu, M.; Saurabh, S.; Gaurav, G.; Dinesh, K. C.; Lakshmi, T.; Kamal, D. *J. Photochem. Photobio*. **2019,** *197*, 111531.